

TABLE

Structures of Apelin and its Analogue

Name	Structure
Apelin-36	
Bovine	LVQPRGPRSGPGPWQGGRRKFRRQRPLSHKGPMMPF
Human	LVQPRGSRNGPGPWQGGRRKFRRQRPLSHKGPMMPF
[pGlu]apelin-13	pERPRLSHKGPMMPF
[pGlu65, Nle75, Tyr77]apelin-13	pERPRLSHKGP(Nle)PY

Figures and Figure Legends

Fig.1. Comparison of human and rat APJ amino acid sequences.

The amino acid sequences of the human (top row) and rat APJ (bottom row) are aligned. Amino acid residues identical in the two species are boxed. Bars indicate the seven predicted transmembrane (TM) regions.

Fig. 2. Tissue distribution of rat *apj* mRNA analyzed by RT-PCR. Poly(A)⁺ RNA preparations obtained from the indicated rat tissues were subjected to quantitative RT-PCR analyses using a ABI Prism 7700 Sequence Detector. Poly(A)⁺RNAs of the placenta and mammary gland were prepared from female rats 17 and 21 days in pregnancy, and those of neonatal tissues were from the rats of 0 to 2 days after birth.

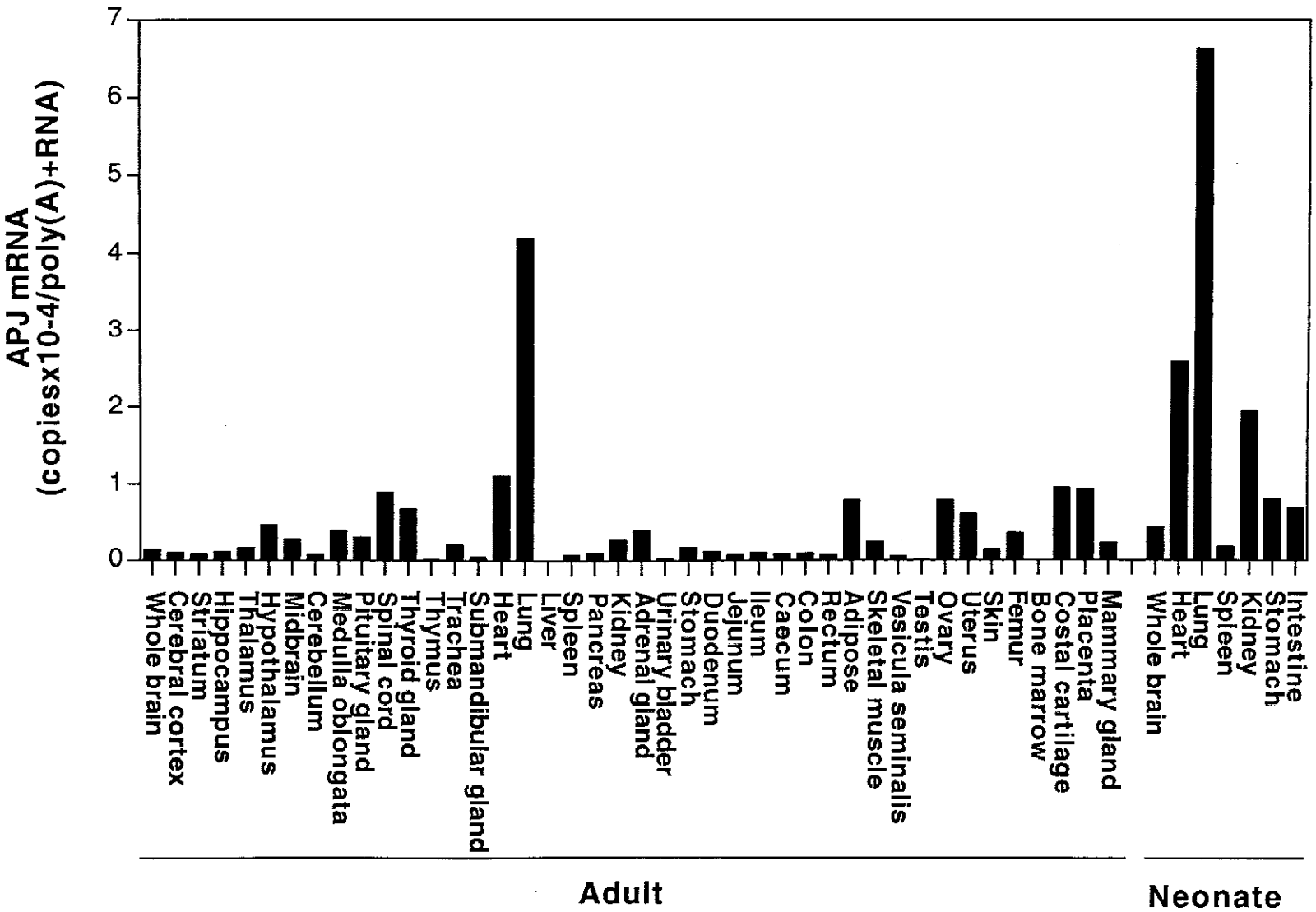


Fig. 3. Comparison of changes in extracellular acidification rates induced by [pGlu]apelin-13 and apelin-36. The acidification rates were measured every 120 s (flow on at 100 μ l/min for 80 s; flow off for 8 s; flow off for 30 s to measure acidification rates). The cells were set in a workstation and exposed to a low-buffered RPMI 1640 medium containing 0.1% BSA until the stable acidification rates were obtained. The cells were stimulated with [pGlu]apelin-13 (A) or apelin-36 (B) dissolved in the medium for 7 min 2 s, corresponding to the cycles 4 to 7 as indicated with a bold bar in the figure. The concentrations of [pGlu]apelin-13 used were 10 (Δ), 1 (\bullet), 0.1 nM (\blacktriangle), and apelin-36 were 100 (\blacksquare), 10 (\triangle) and 1 nM (\bullet), respectively. The acidification rates of the cells without apelin were also shown as (\circ). The basal acidification rates in the first 3 cycles were normalized to 100%.

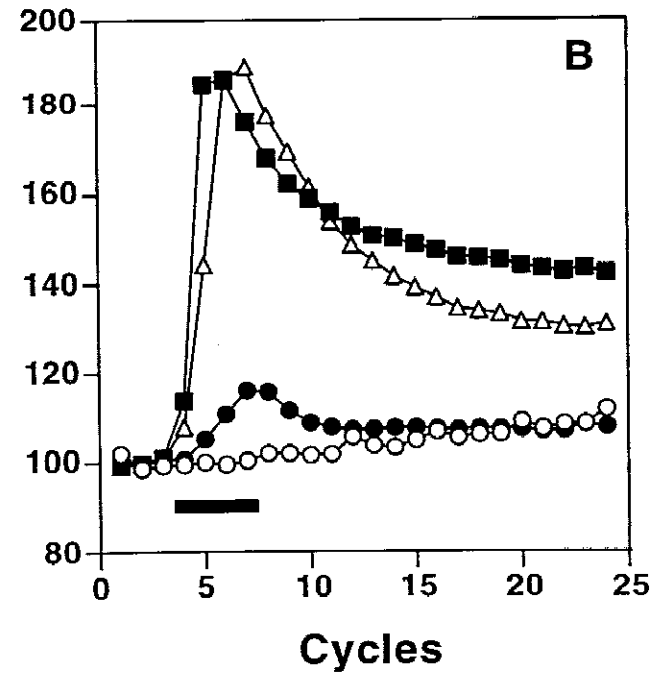
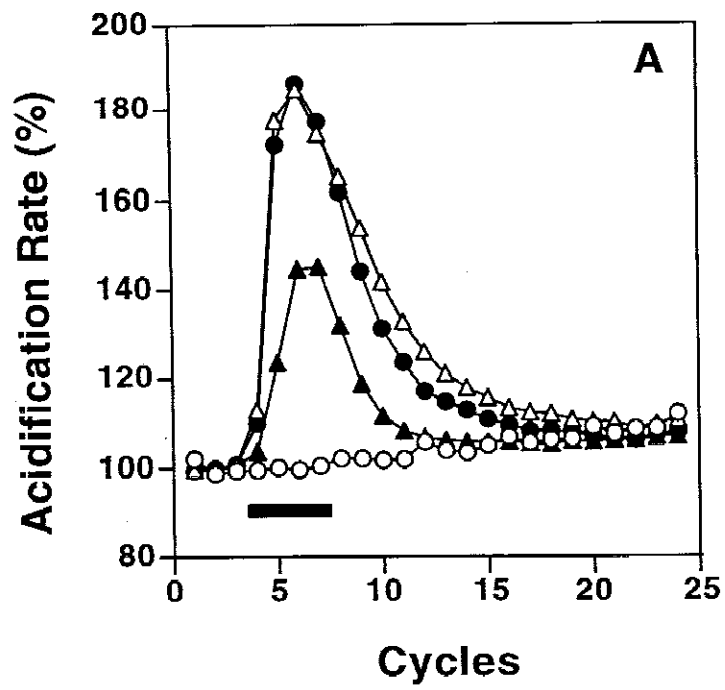


Fig. 4. Effects of PTX treatment on cellular acidification rates. CHO-A10 cells cultured in capsules were incubated with (●) or without (○) 100 ng/ml PTX for 24 h, prior to the measurement. The cells were then set in the workstation and exposed a low-buffered RPMI 1640 medium containing 0.1% BSA until the stable acidification rates were obtained. The cellular acidification rates were measured as described in the legend of Fig. 5. The cells were stimulated with 100 nM of [pGlu]apelin-13 (A) or apelin-36 (B) for 7 min 2 s, corresponding to cycles 4 to 7 as indicated with a bold bar in the figures. The basal acidification rates in the first 3 cycles were normalized to 100%.

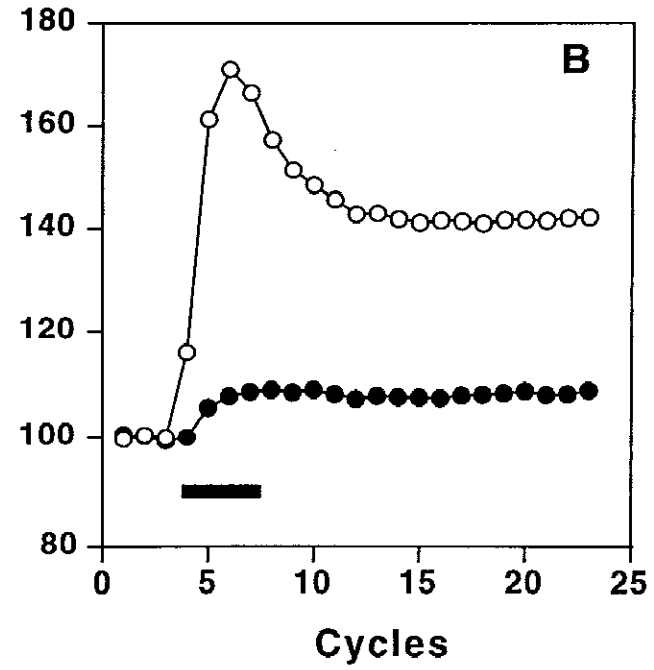
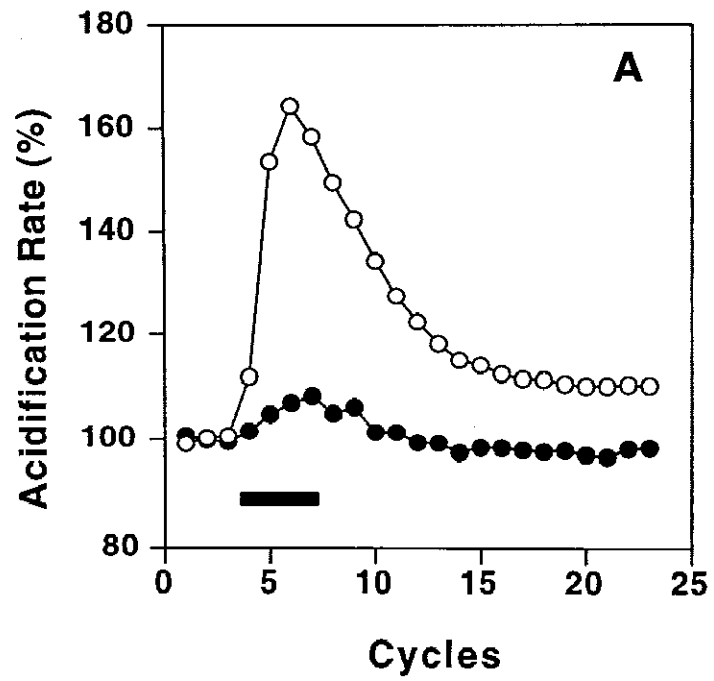


Fig. 5. Effects of MIA treatment on cellular acidification rates. CHO-A10 cells set in a workstation were exposed a low-buffered RPMI 1640 medium containing 0.1% BSA, and cellular acidification rate was measured as described in the legend of Fig. 5. The running media were replaced with the medium with (●) or without (○) 10 μ M of MIA, and the cells were incubated until stable acidification rates were obtained. Then the cells were stimulated with 100 nM of [pGlu]apelin-13 (A) or apelin-36 (B) for 7 min 2 s, corresponding to cycles 4 to 7 as indicated with a bold bar in the figures. The basal acidification rates in the first 3 cycles were normalized to 100%.

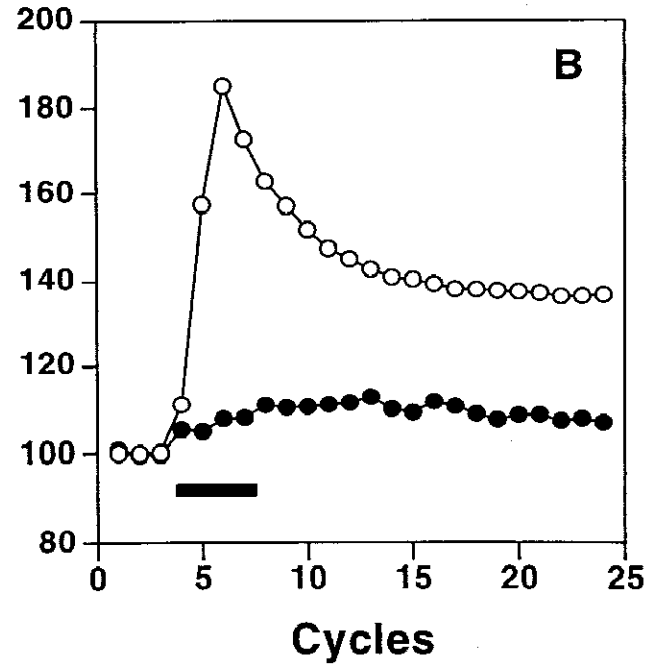
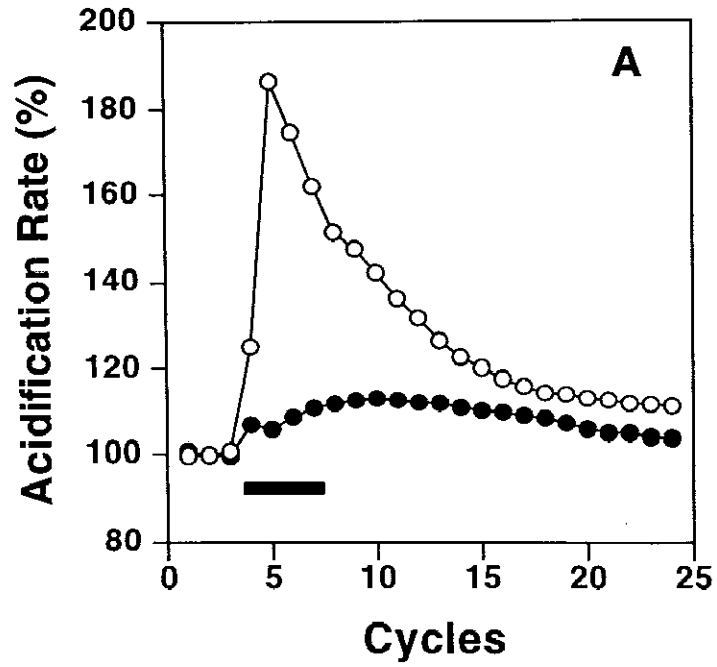


Fig. 6. Scatchards analysis of radiolabeled apelin binding to APJ. The membrane preparations of CHO-A10 cells ($1 \mu\text{g}/100 \mu\text{l}$) were incubated with the increasing concentrations of [^{125}I][pGlu65,Nle75,Tyr77]apelin-13 at room temperature. The bound and free ligands were separated at the time when the binding of [^{125}I][pGlu65,Nle75,Tyr77]apelin-13 became equilibrium (90 min). The amounts of nonspecific binding were estimated by adding $1 \mu\text{M}$ of unlabeled [pGlu65,Nle75,Tyr77]apelin-13 to the reaction. Data are plotted as bound (B, pmol mg^{-1}) versus the bound/free (B/F, $\text{pmol mg}^{-1} \text{nM}^{-1}$) radio-labeled ligands. Each symbol represents the mean value with standard error in triplicate determinations.

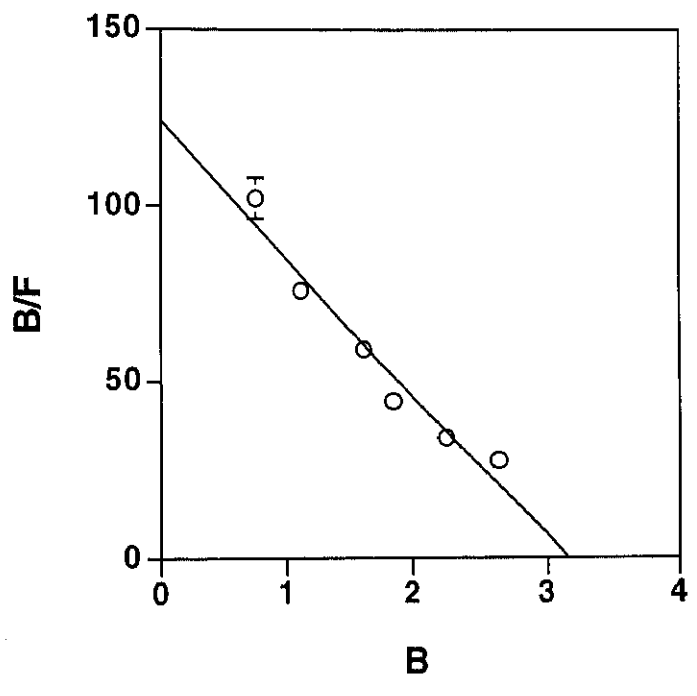


Fig. 7. Competitive inhibition of radio-labeled apelin binding to APJ by [pGlu]apelin-13 and apelin-36. The competitive inhibition of [¹²⁵I][pGlu65,Nle75,Tyr77]apelin-13 (100 pM) binding to the membrane preparations of CHO-A10 cells (0.25 μg/100 μl) was examined at the indicated concentrations of [pGlu]apelin-13 (○) and apelin-36 (●), respectively. The bound and free ligands were separated after the incubation for 90 min at room temperature. The amounts of nonspecific binding were estimated by adding 1 μM of unlabeled [pGlu65,Nle75,Tyr77]apelin-13 to the buffer. Each symbol represents the mean value in triplicate determinations. Standard error bars are invisible because they lie inside in the symbols.

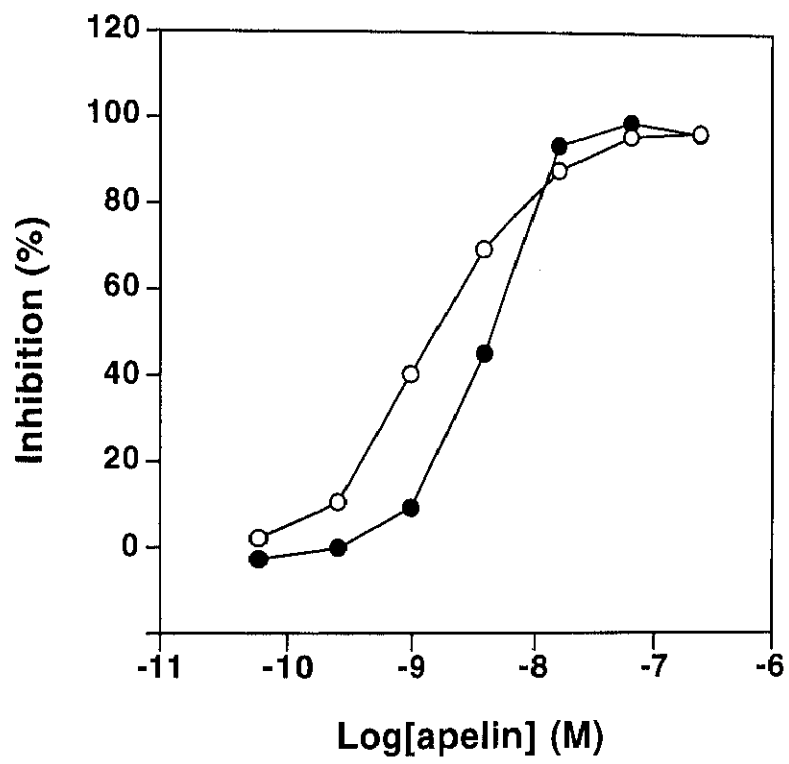


Fig. 8. Binding of radio-labeled apelin to CHO-A10 cells treated with [pGlu]apelin-13 or apelin-36. A, The time-course of association of [¹²⁵I][pGlu65,Nle75,Tyr77]apelin-13 to intact CHO-A10 cells. CHO-A10 cells cultured in 24-well tissue culture plates were incubated with 200 pM of [¹²⁵I][pGlu65,Nle75,Tyr77]apelin-13 at room temperature for the indicated time. The unbound ligands were removed by washing the cells with the buffer, and radioactivities remained on the cells were harvested by lysing the cells with NaOH-SDS solution and measured. The amounts of nonspecific binding were estimated by adding 1 μ M of unlabeled [pGlu65,Nle75,Tyr77]apelin-13 to the buffer. B, The binding of [¹²⁵I][pGlu65,Nle75,Tyr77]apelin-13 to CHO-A10 cells pretreated with [pGlu]apelin-13 or apelin-36. CHO-A10 cells were incubated with 1 μ M of [pGlu]apelin-13 (○, ●) or apelin-36 (△, ▲) for 90 min at room temperature. After the unbound peptides were removed by washing the cells with the buffer, the binding of [¹²⁵I][pGlu65,Nle75,Tyr77]apelin-13 were examined as described above. The amounts of nonspecific binding (●, ▲) were estimated by adding 1 μ M of unlabeled [pGlu65,Nle75,Tyr77]apelin-13 to the buffer. Each symbol represents the mean value with standard error in triplicate determinations.

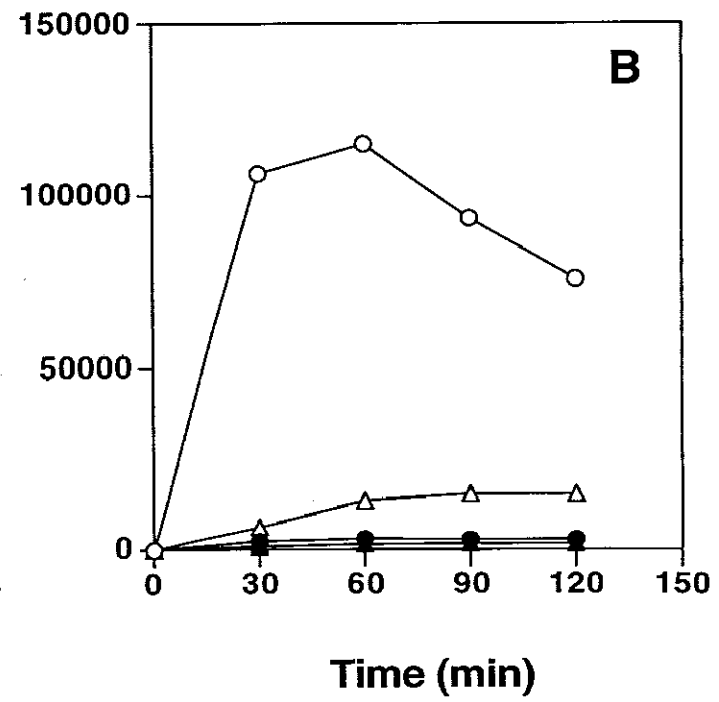
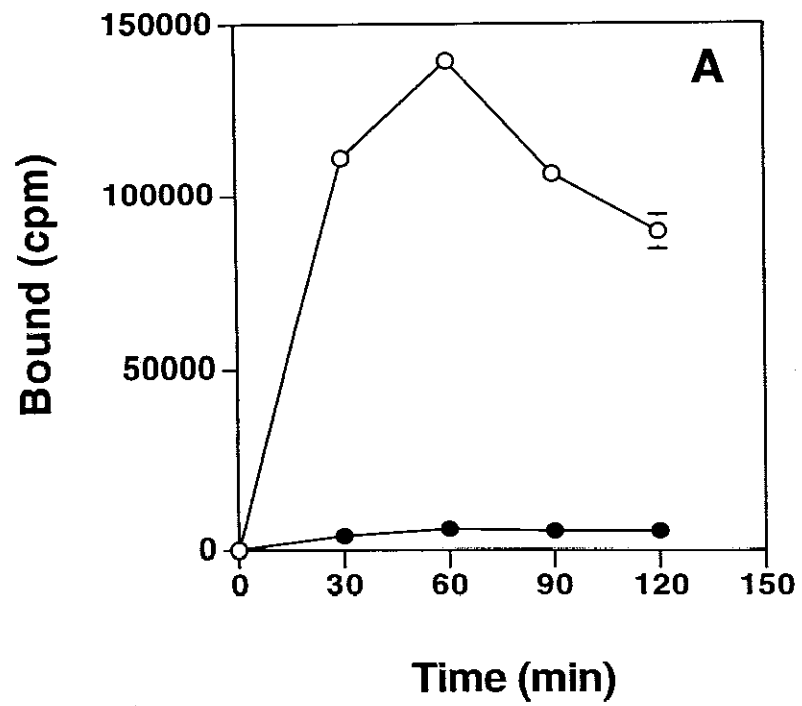


Fig. 9. Chemotaxis of CHO-A10 cells by [pGlu]apelin-13 and apelin-36. CHO-A10 cells (open symbols) and mock transfected CHO cells (closed symbols) were incubated with the indicated concentrations of [pGlu]apelin-13 (○, ●) and apelin-36 (△, ▲) in 96-well microchemotactic chamber at 37 °C for 4 h. After being fixed, the cells were stained with Diff-Quick, and the number of migrating cells was estimated by absorbance at 595 nm. Each symbol represents the mean value with standard error in triplicate determinations.

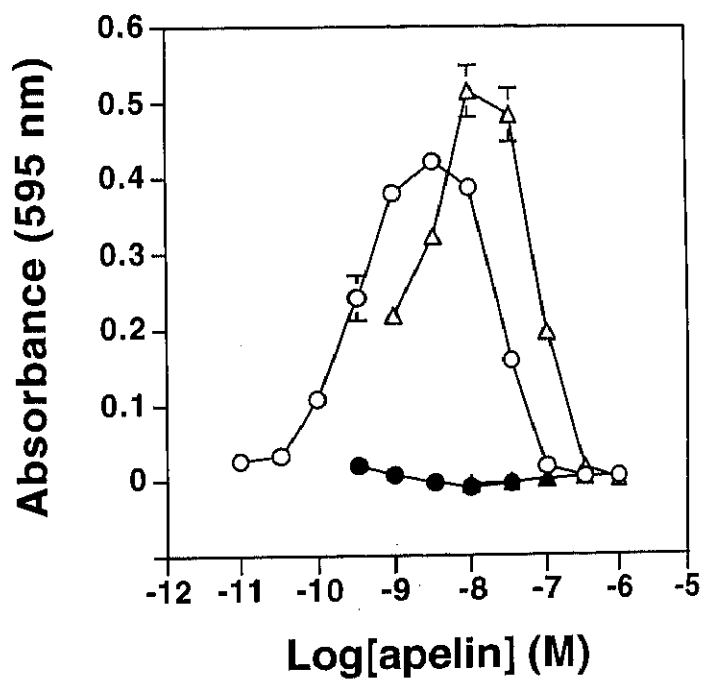


Fig. 10. Gel filtration chromatography of bovine colostrum. The peptide-enriched fraction prepared from bovine colostrum was analyzed by gel filtration chromatography. Apelin contained in each fraction was detected by the forskolin-stimulated cAMP production-inhibitory assay. The positions of synthetic apelin-36 and [pGlu]apelin-13 eluted in the same chromatography were indicated with arrows in the figure.

